

# Raman spectroscopy in high-pressure research

*Sergei GORYAINOV*

*Sobolev Institute of Geology and Mineralogy SB RAS, Novosibirsk, Russia*

---

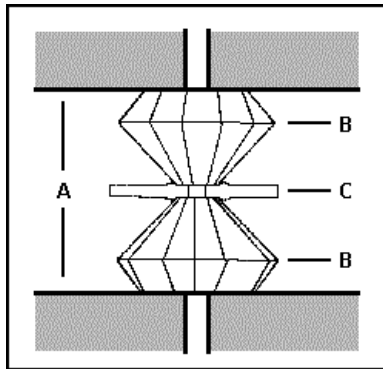
**Lecture as the review of series of research works carried out by the group:**

*1 Goryainov S.V., 2 Krylov A.S., 1 Likhacheva A.Yu., 1 Rashchenko S.V. , 2 Vtyurin A.N.*

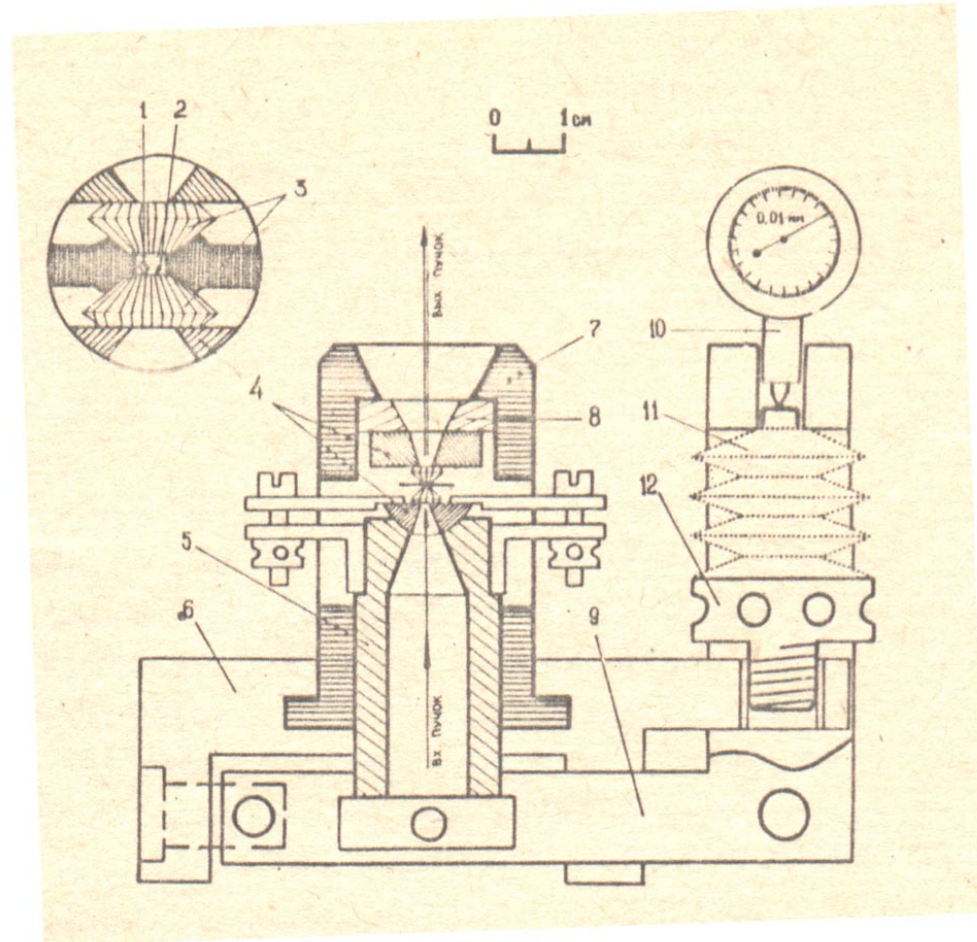
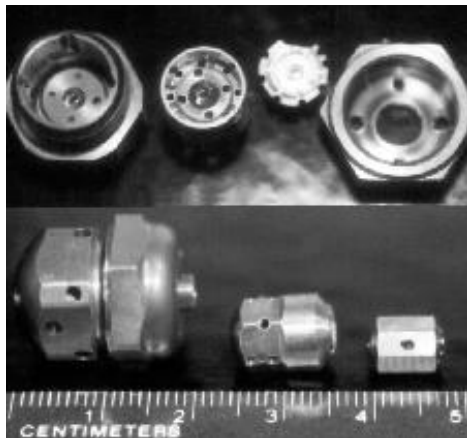
**In-situ Raman study of minerals at high pressure in diamond anvil cell: methods and achievements**

- *1- Sobolev Institute of Geology and Mineralogy SB RAS, pr. Koptyug 3, Novosibirsk, Russia*
- *2- Kirensky Institute of Physics SB RAS, Akademgorodok, Krasnoyarsk, Russia*

# Diamond anvil cell DAC



Scheme of DAC: A-solid supports,  
B-anvils, C- gasket



DAC cells, loaded with one or several screws:

- cell with one screw;
- cell with three screws;
- cell with lever arm and one screw.

- Raman spectrometers were used:
- Dilor OMARS 89,
- Horiba Jobin Yvon LabRam-HR800 and T64000,
- Spex Triplemate, Renishaw Model 2000 RS
  
- Suitable gasket materials are hardened stainless-steel, tungsten, rhenium, inconel nickel alloy etc.
- Medium: alcohol (methanol/ ethanol 4/1), water, KBr, glycerol etc.
  
- P-indicators: ruby (R1 and R2 lines), Sm-borate

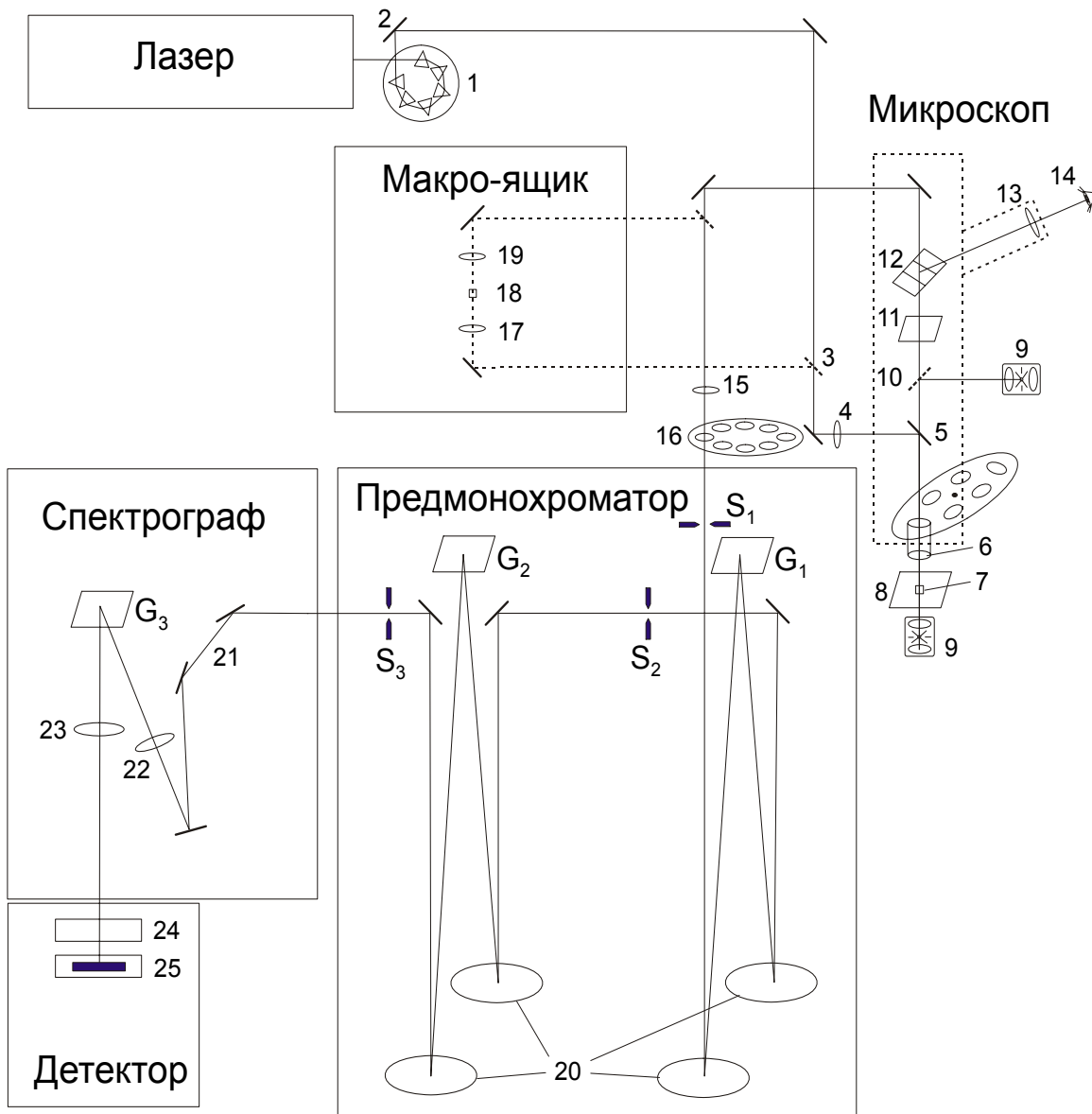


Fig. Scheme of Raman spectrometer (Dilor OMARS 89)



Horiba JobinYvon T64000

Raman spectrometer

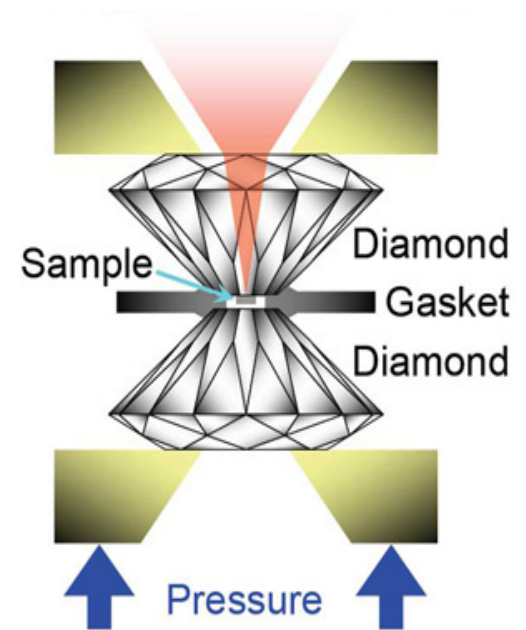


- Horiba JobinYvon LabRam HR800 Raman spectrometer with DAC (IGM)



## DAC at high P-T:

Raman equipment Horiba Jobin Yvon T64000 spectrometer with Olympus BX41 microscope with attached heated cell HT-DAC, EasyLab  $\mu$ Scope .



# Minerals at high pressure

- Using Raman spectroscopy in DAC-diamond anvil cell, several minerals were investigated at high P and room T:
  - 1. Natrolite [20]
  - 2. Thomsonite [13]
  - 3. Scolecite [13]
  - 4. Zeolite NaA [15]
  - 5. Lawsonite [19]
  - 6. H<sub>2</sub>O-cordierite [14]
  - 7. Fluorapatite [20]
  - 8. OH-apophyllite [7]
  - 9. F- apophyllite [7]
  - 10. Thaumassite [28]
  - 11. Datolite [8]
  - 12-13. Dehydrated and Hydrated analcimes
    - 14. Parasibirskite [29]; 15 Chibaite [25].



- Dependences  $\nu(P)$  of stretching modes versus pressure can be estimated from potential model (Sherman, 1982) [18]:
- $U(r) = A - Br^{-n} + Cr^{-m}$ ,
- where  $A, B, C, n$  (in power),  $m$  (in power) – constants,  $r$  – inter-atomic distance.
- Effective force constant depends on  $r$  with rate:  $dk/dr = -(n + m + 3)k_0/r_0$ ,
- where  $k_0, r_0$  – constants are found at 0-pressure.
- Hence, for materials with Lennard-Jones potential ( $n = 6, m = 12$ ):
- $dk/k_0 = -21 dr/r_0$ ,
- that means the increase of force constant 21% at the decrease of inter-atomic distance 1%
- In alkali halides for ionic potential of 1-9 type ( $n = 1, m = 9$ ):
- $dk/k_0 = -13 dr/r_0$
- that means the increase of force constant 13% at the decrease of inter-atomic distance 1%.

- Using the noted potential, the band frequency versus  $P$  can be estimated by complex formula (Sherman, 1982) [18]. From that, hence, the dependence  $\nu(P)$  is linear at small  $P$  and then  $\nu(P)$  is nonlinear at large  $P$  with decreasing of the slope  $d\nu/dP$ .
- At zero pressure, the slope  $d\nu/dP$ :
- $$(d\nu/dP)_0 = \nu_0 (n+m+3)/6K_0,$$
- where  $K_0$  is the bulk modulus,  $r_0$  and  $\nu_0$  at  $P=0$ . Curvature of the  $P$ -dependence of  $\nu(P)$  is expressed:
- $$(d^2\nu/dP^2)_0 = -\nu_0 (m^2 + 14m + 14n + 4mn + n^2 + 29)/36(K_0)^2.$$

# Hydrated NATROLITE

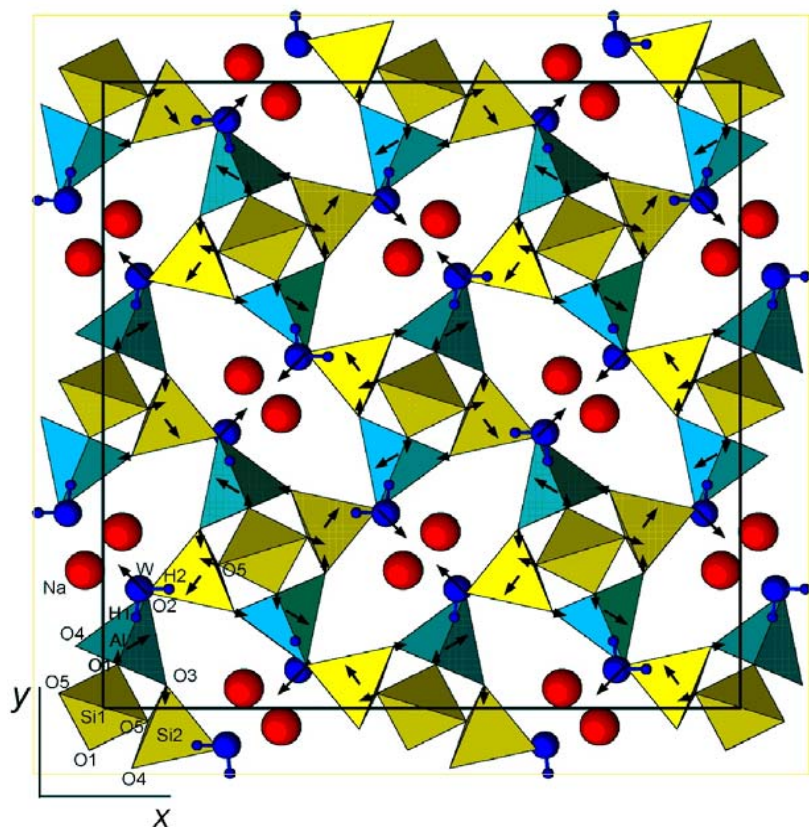


Fig. Crystal structure of initial phase of natrolite  $\text{Na}_2\text{Al}_2\text{Si}_3\text{O}_{10} \cdot 2\text{H}_2\text{O}$ . Strong mode at  $443 \text{ cm}^{-1}$

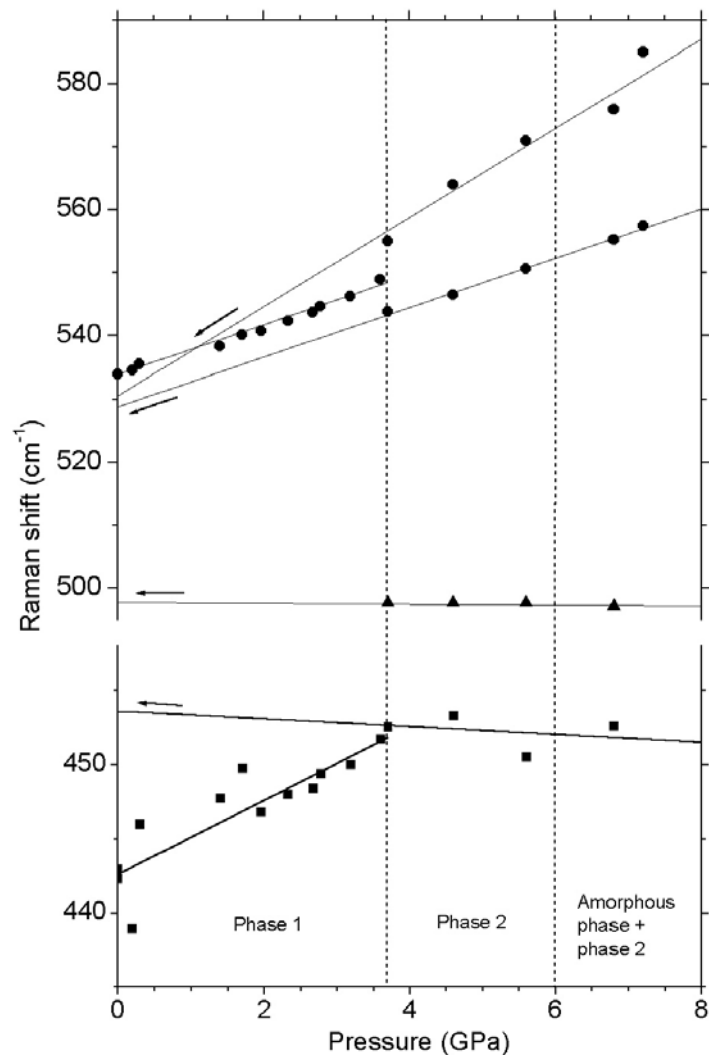
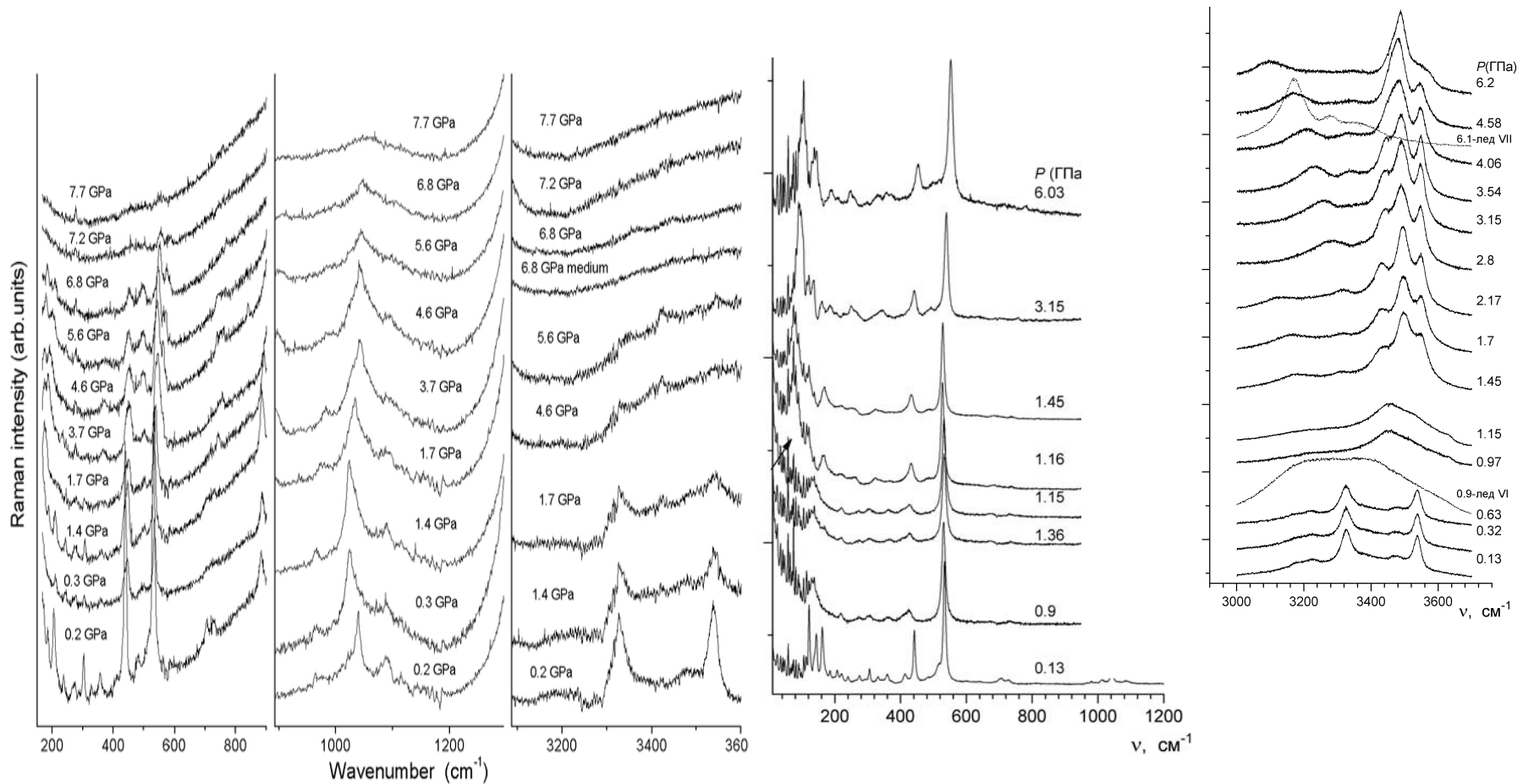


Fig. Baric dependence of wavenumber of natrolite Raman bands. Amorphization at 9 GPa and partial reconstruction of crystalline structure after decompression..

# Hydrated and overhydrated natrolite at high pressure (Raman spectra with increasing $P$ )



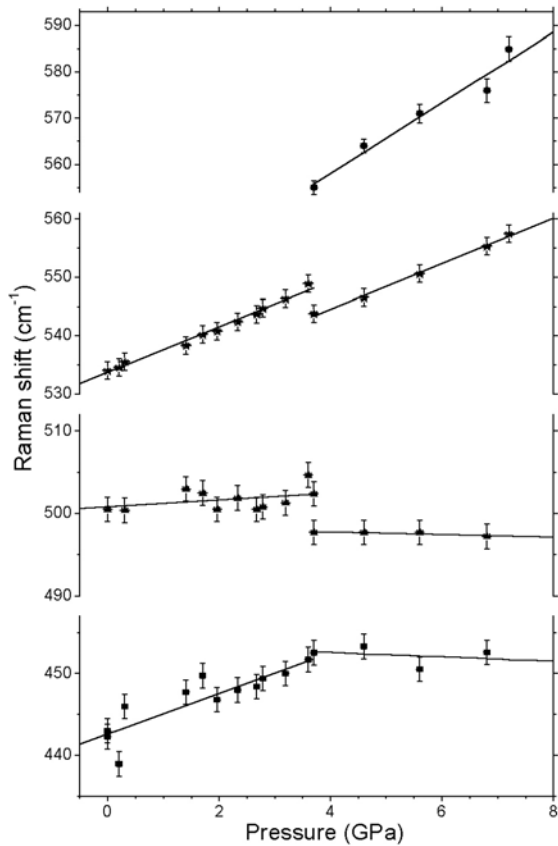
Hydrated natrolite starting from initial phase

Overhydrated natrolite starting from initial phase

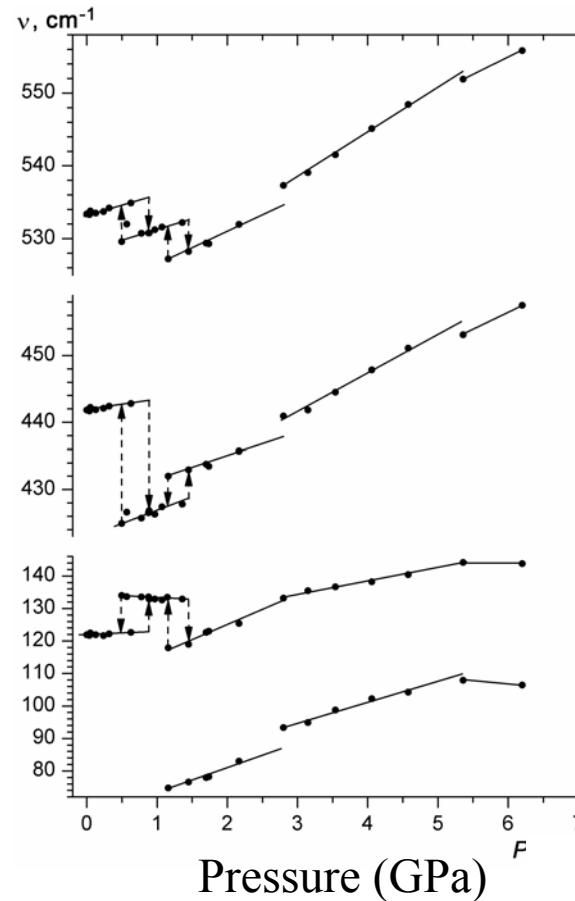
# Overhydrated zeolites

Earlier data on overhydration of zeolites are presented in ref. [10-12,16].

Hydrated and overhydrated zeolite natrolite at high pressure. Our data [20].  
Baric dependence of wavenumbers of the Raman bands



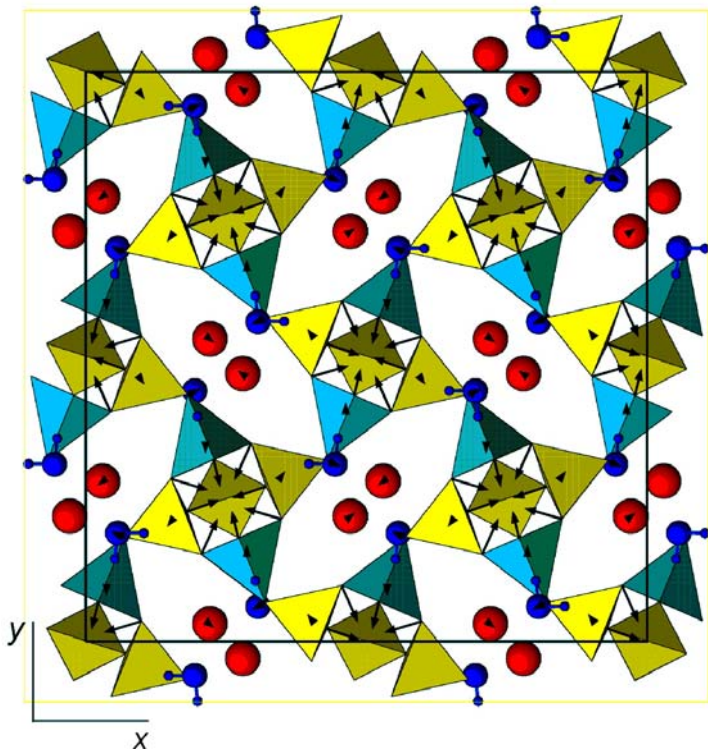
Hydrated



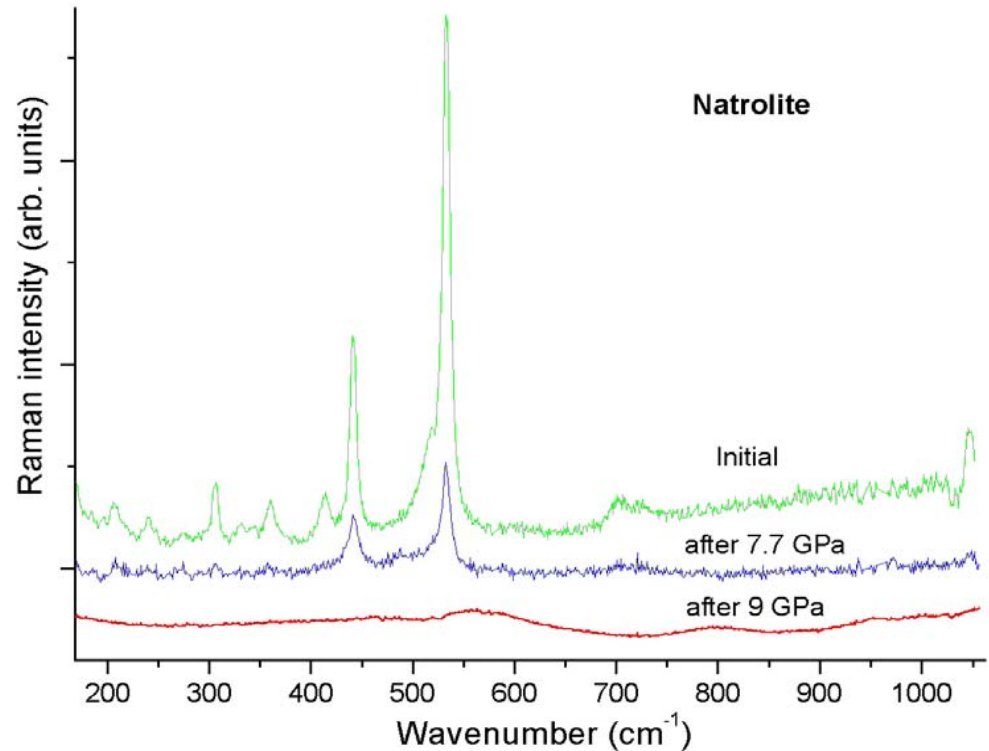
Overhydrated

# Natrolite

Reversibility of amorphization at compression up to 7.7 GPa  
Irreversibility of amorphization at compression up to ~9 GPa.



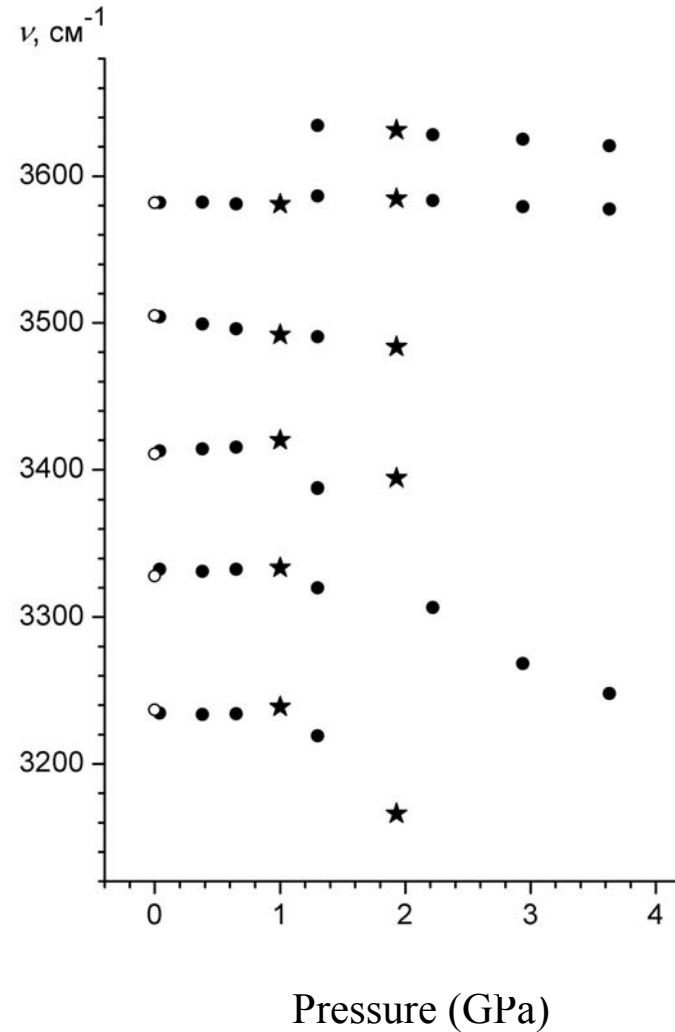
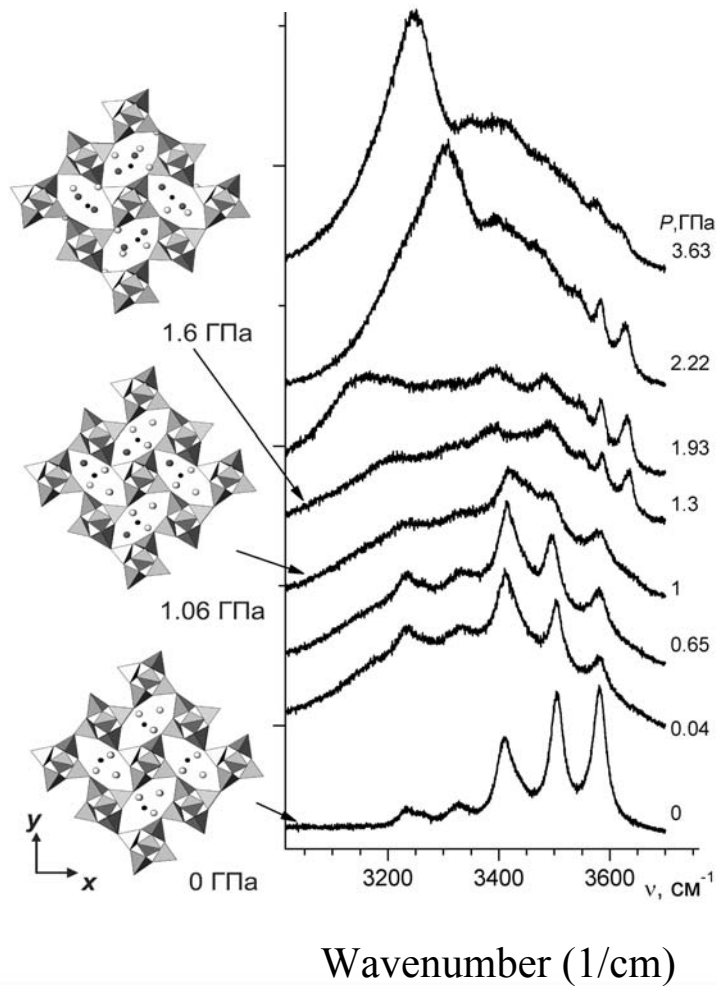
Initial crystalline structure of natrolite  $\text{Na}_2\text{Al}_2\text{Si}_3\text{O}_{10} \cdot 2\text{H}_2\text{O}$ .  
Mode vibration at  $534 \text{ cm}^{-1}$ .



Raman spectra of natrolite  
 $\text{Na}_2\text{Al}_2\text{Si}_3\text{O}_{10}$

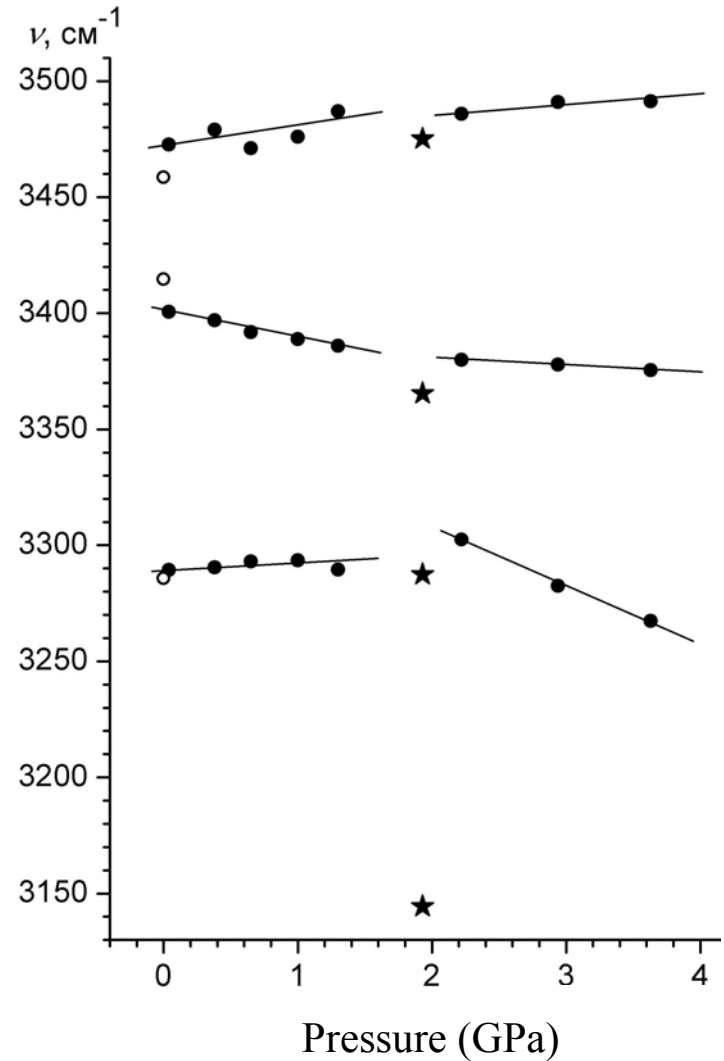
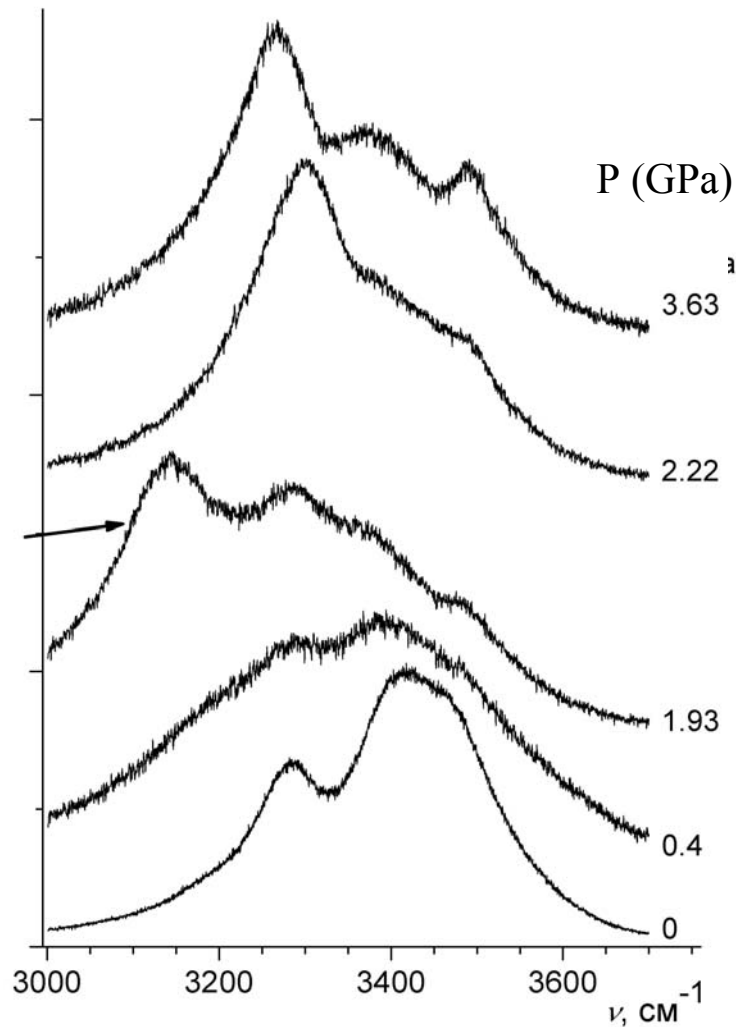
# Overhydrated zeolite scolecite at high pressure

(Raman spectra with increasing  $P$ ). Our data [13].



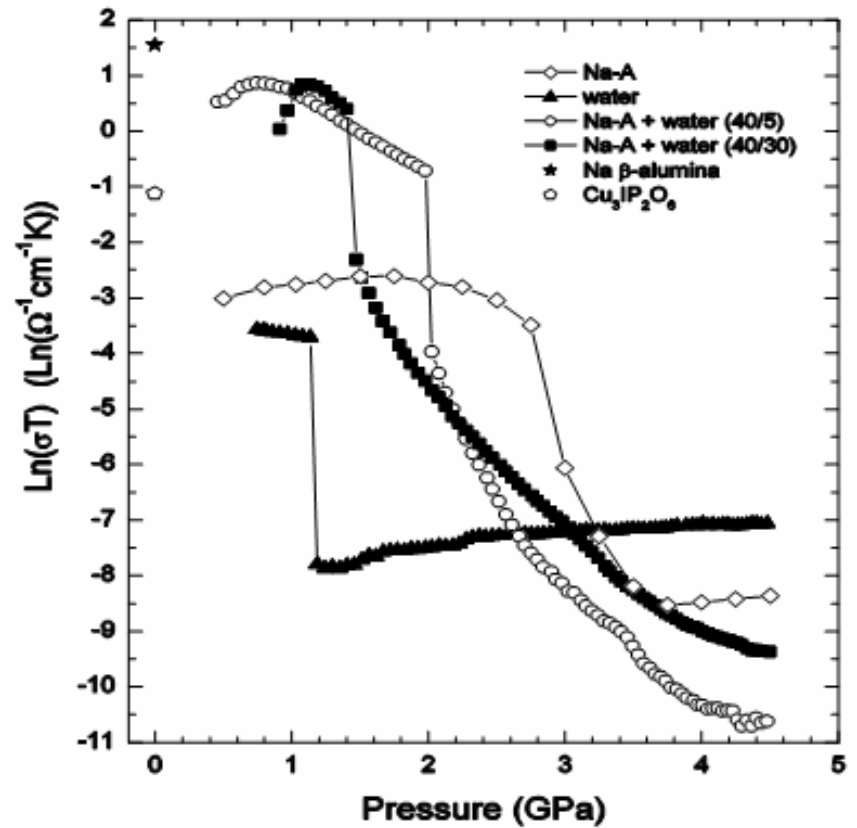
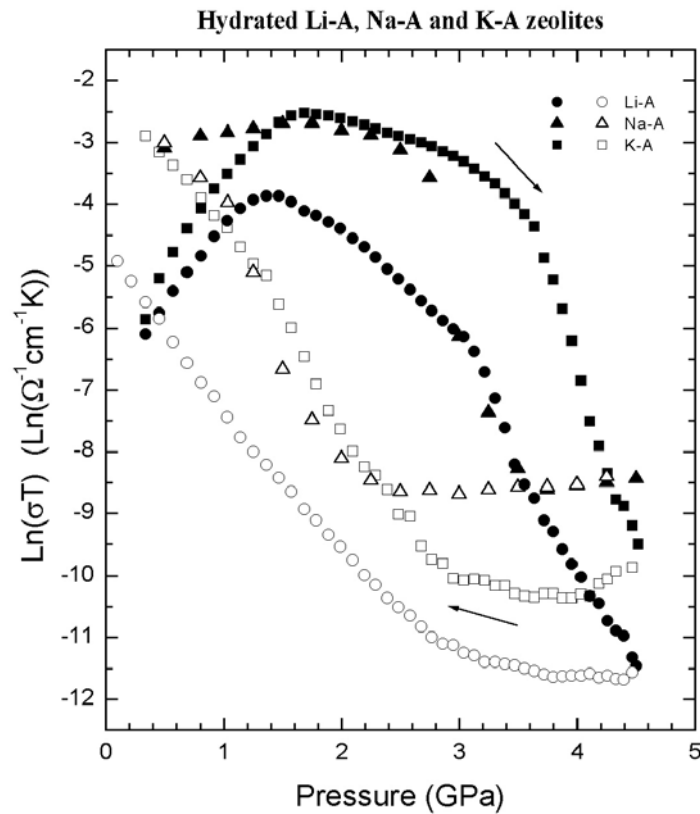


Overhydrated zeolite thomsonite at high pressure  
(Raman spectra with increasing P). Our data [13].



# Ionic conductivity of overhydrated zeolite NaA

Ionic conductivity of hydrated zeolites: LiA, NaA and KA



## NaA overhydrated zeolite:

ionic conduction (our data, Goryainov et al., *Micropor. Mesopor. Mater.* 2013 [15]) and calculated structure (Peral, Iniguez, *Phys. Rev. Lett.* 2006.)

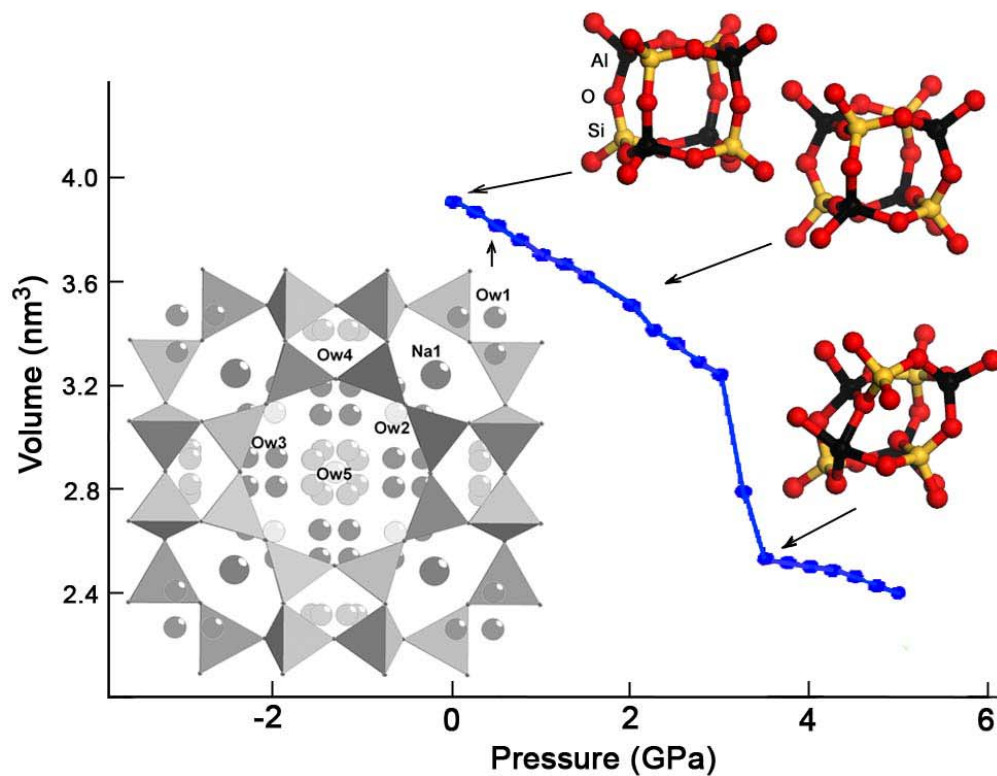
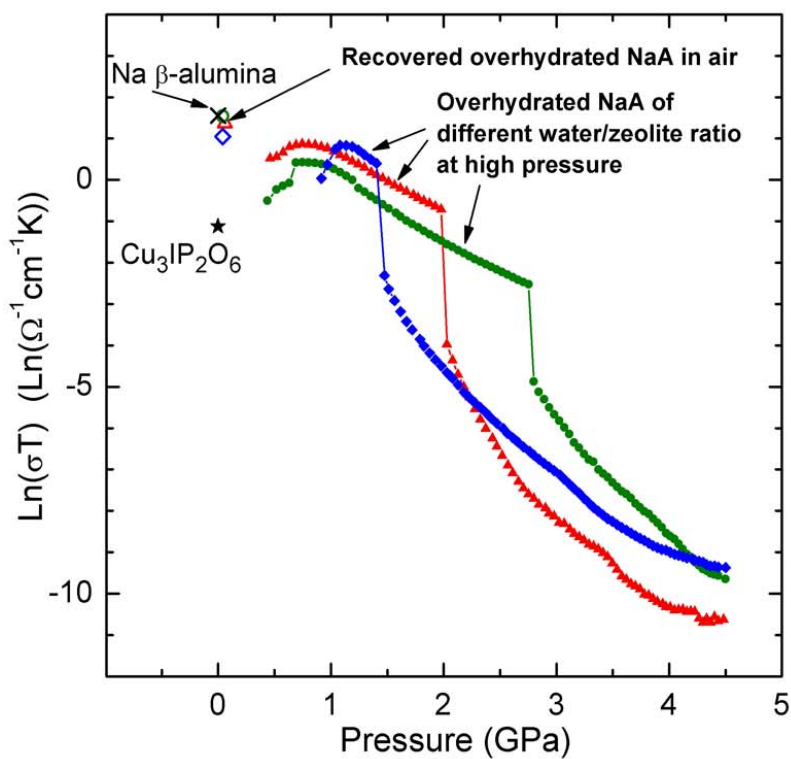
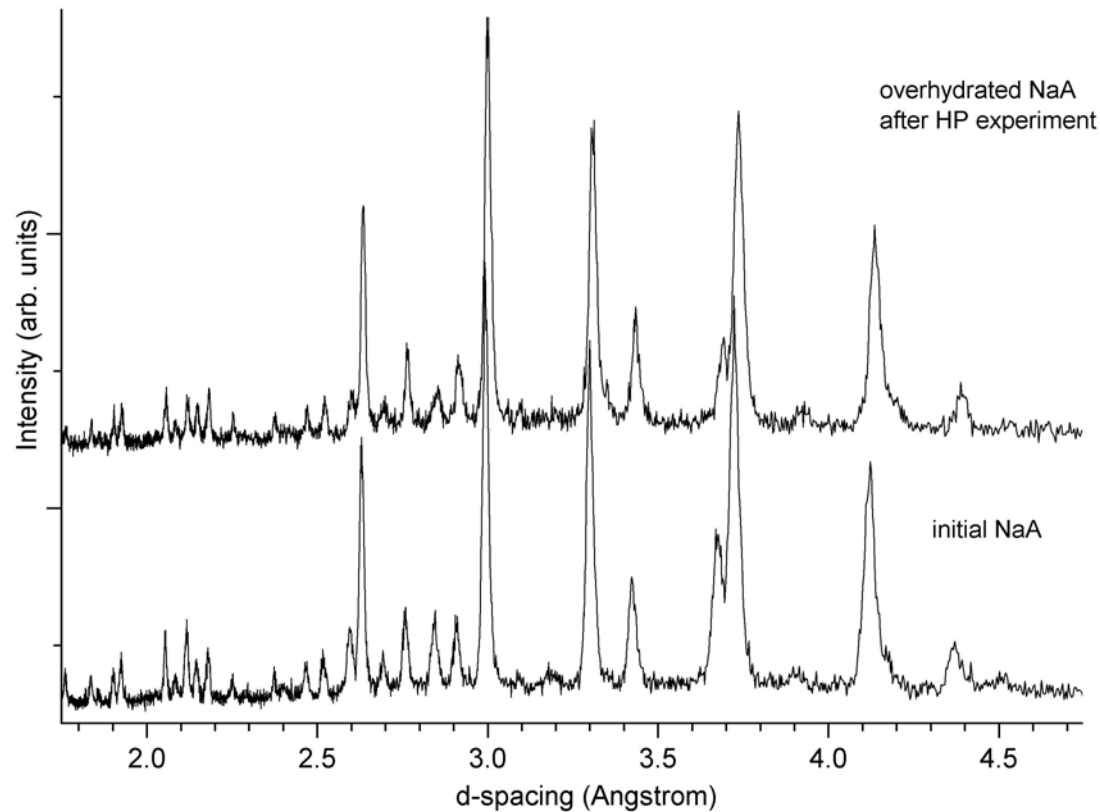


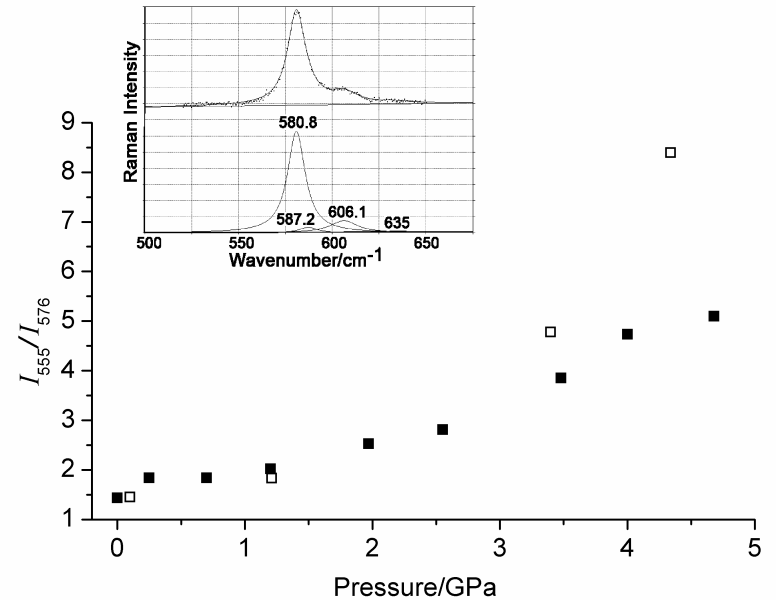
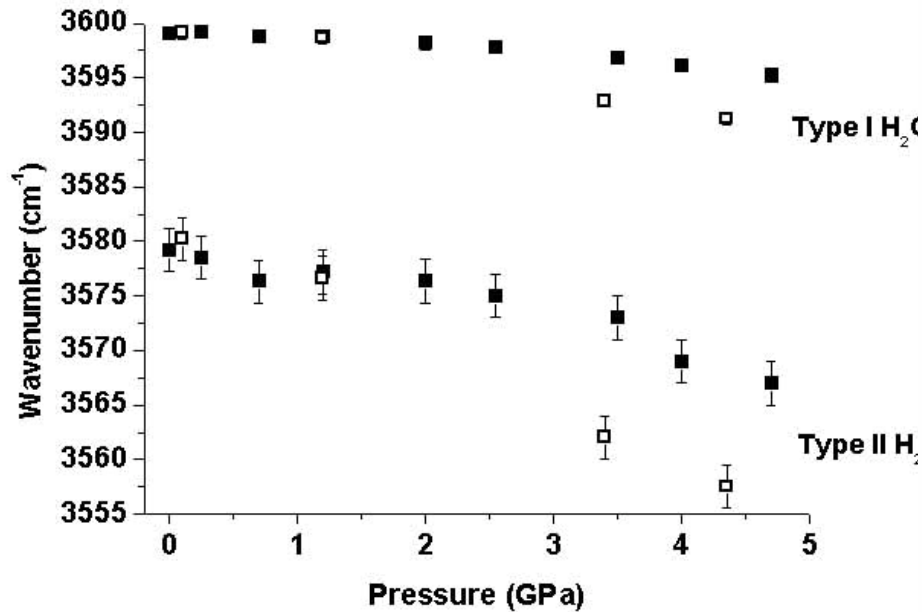
Fig. NaA zeolite XRD: initial (lower) and overhydrated (upper) zeolite, proved the conservation of partly overhydrated state for 12 h.



## H<sub>2</sub>O-cordierite (Altai mountains)

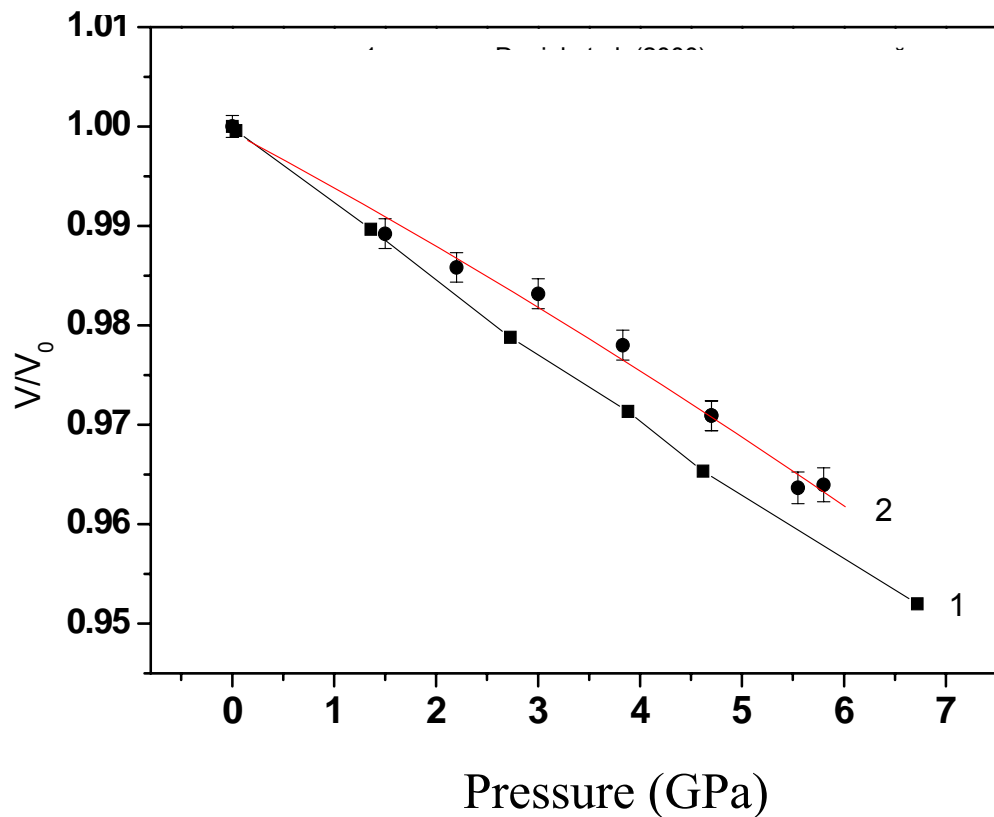
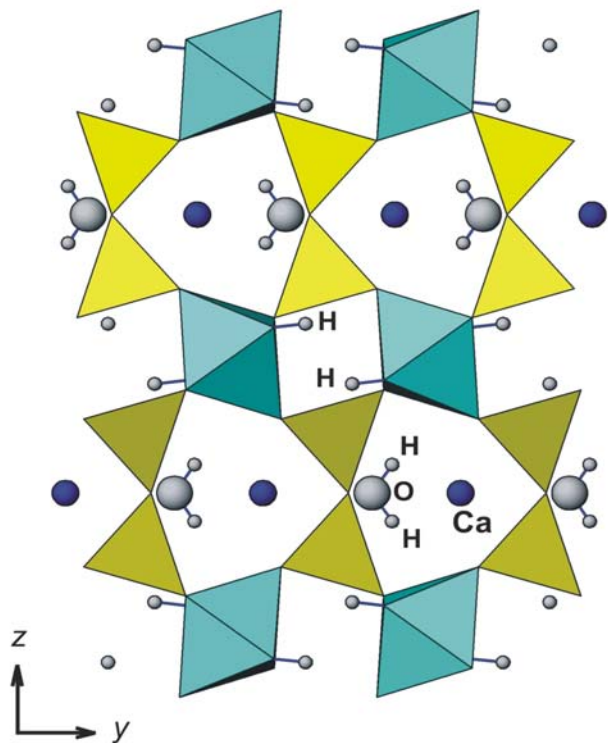
Na<sub>0.07</sub>(Mg<sub>1.57</sub>Fe<sub>0.36</sub>Mn<sub>0.07</sub>) [Al<sub>3.96</sub>Fe<sub>0.06</sub>Si<sub>4.98</sub>O<sub>18</sub>]\*0.45H<sub>2</sub>O

Sample compressed in water. Raman data [14].



# Lawsonite $\text{CaAl}_2\text{Si}_2\text{O}_7(\text{OH})_2 \cdot \text{H}_2\text{O}$ compressed in water and alcohol. X-ray diffraction [19]

Compressibility of lawsonite measured with synchrotron X-ray diffraction. 1- data of Daniel et al. (2000) [27] (black squares), compression in alcohol; 2- our data [19] (black circles), compression in water with alcohol admixture (water/ethanol 9/1). Lines are the approximations of the data.



Lawsonite  $\text{CaAl}_2\text{Si}_2\text{O}_7(\text{OH})_2 \cdot \text{H}_2\text{O}$  compressed in water and alcohol.  
Raman and X-ray diffraction data 2009 [19].

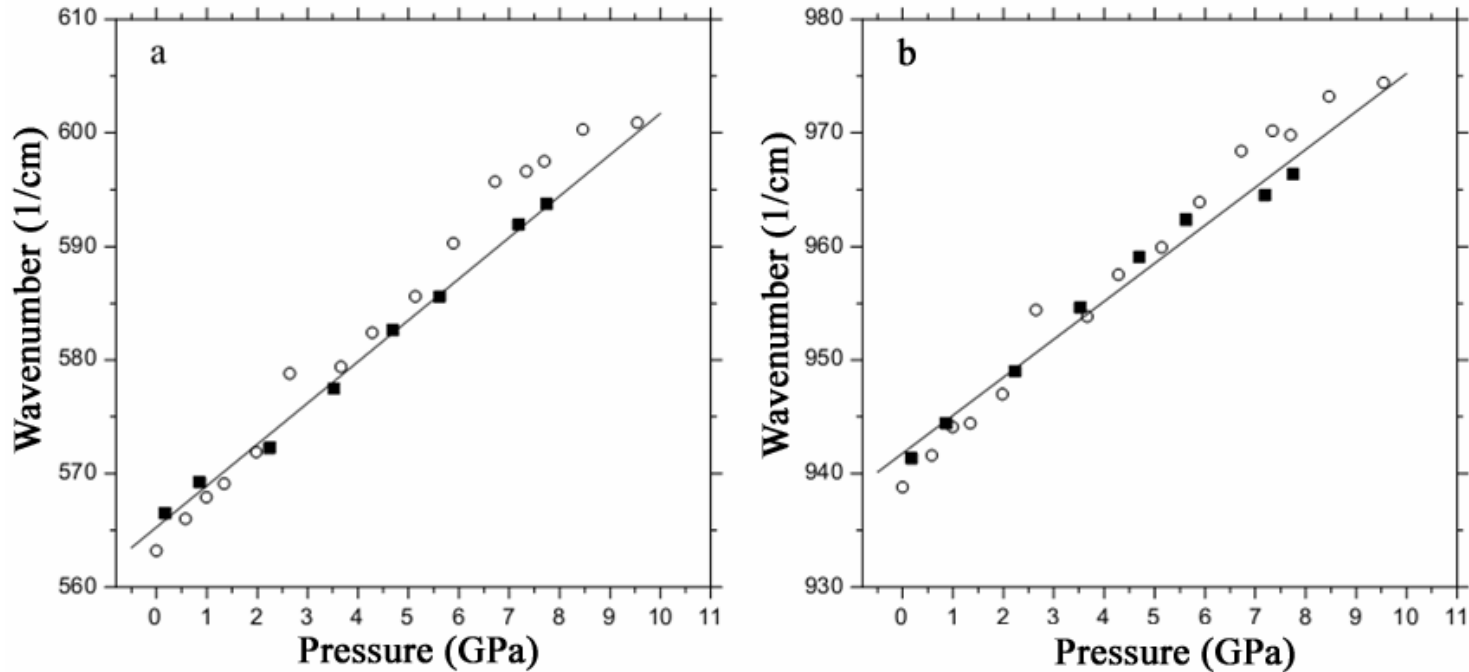
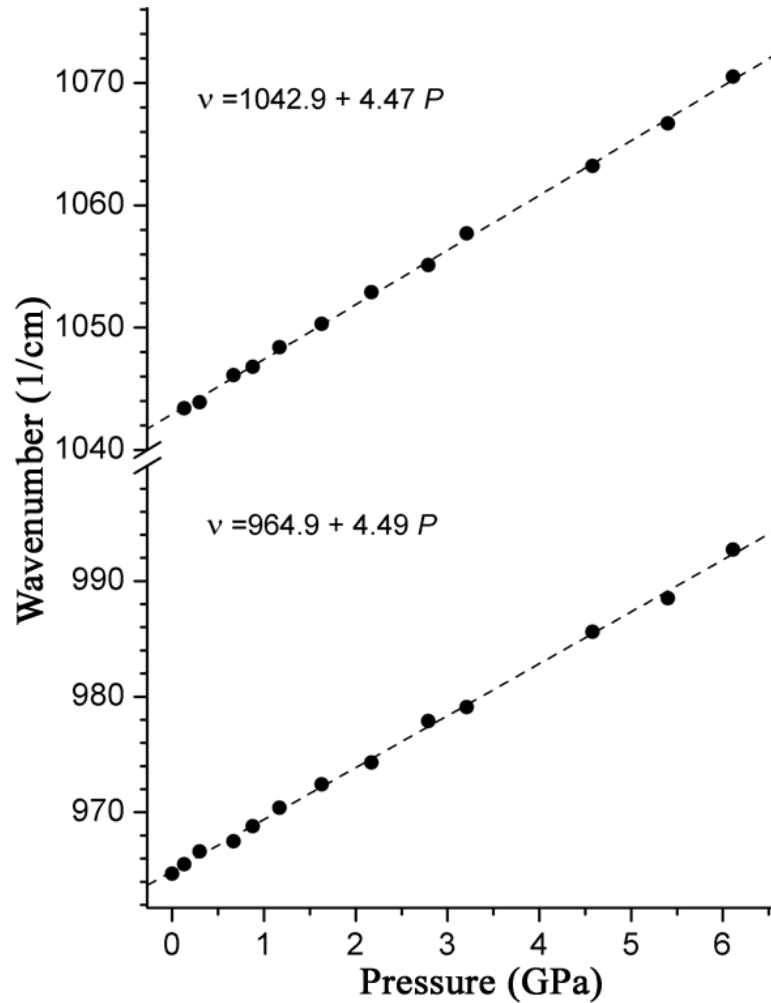


Fig. Pressure dependence of wavenumbers of lawsonite  $\text{CaAl}_2\text{Si}_2\text{O}_7(\text{OH})_2 \cdot \text{H}_2\text{O}$  Raman bands at 566 (a) and 941  $\text{cm}^{-1}$  (b). Lawsonite crystals are compressed in water (circles) and methanol-ethanol 4:1 medium (squares). Linear approximation of experimental points for the last medium is plotted.

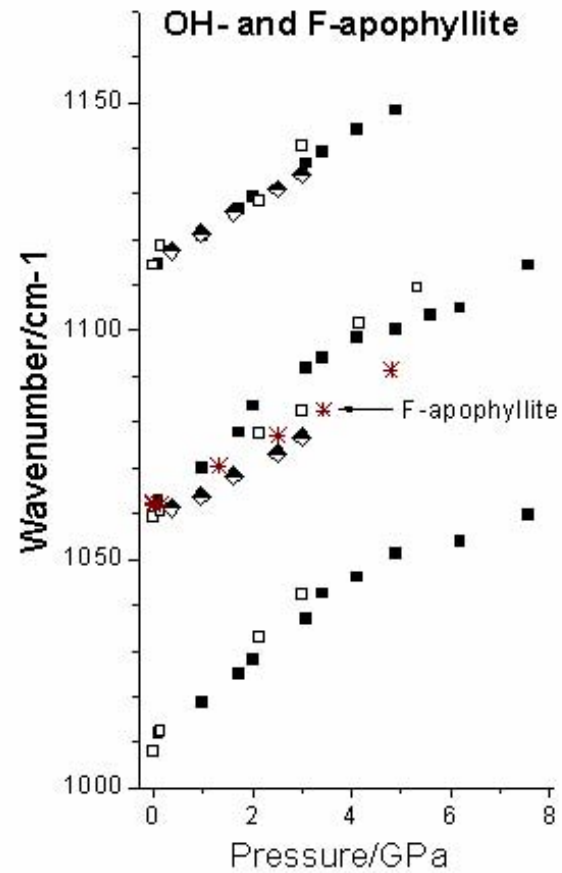
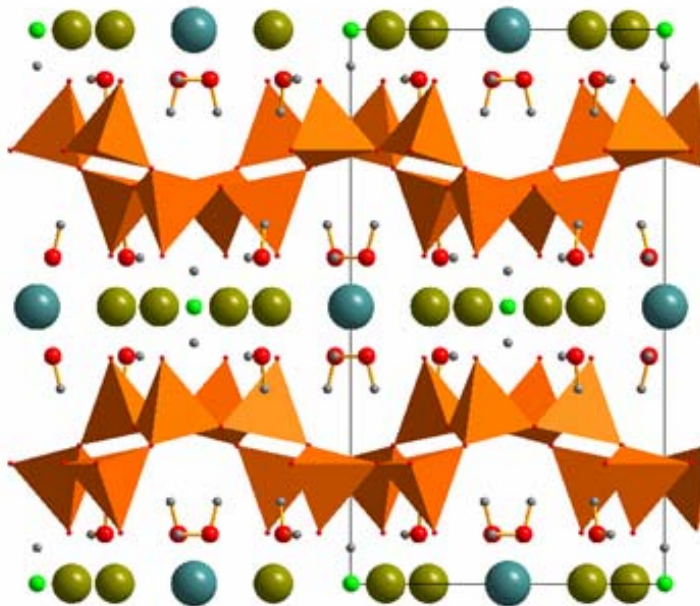


# F-apatite compressed in water.

Raman data [20].



F-apophyllite  $\text{KCa}_4\text{Si}_8\text{O}_{20}(\text{F}, \text{OH}) \cdot 8\text{H}_2\text{O}$  compressed in alcohol.  
Raman data (Goryainov et al., J. Raman Spec. 2012) [7].



- **Raman method at high P-T conditions**
- **Minerals: wairakite, dawsonite, talc and thaumasite**

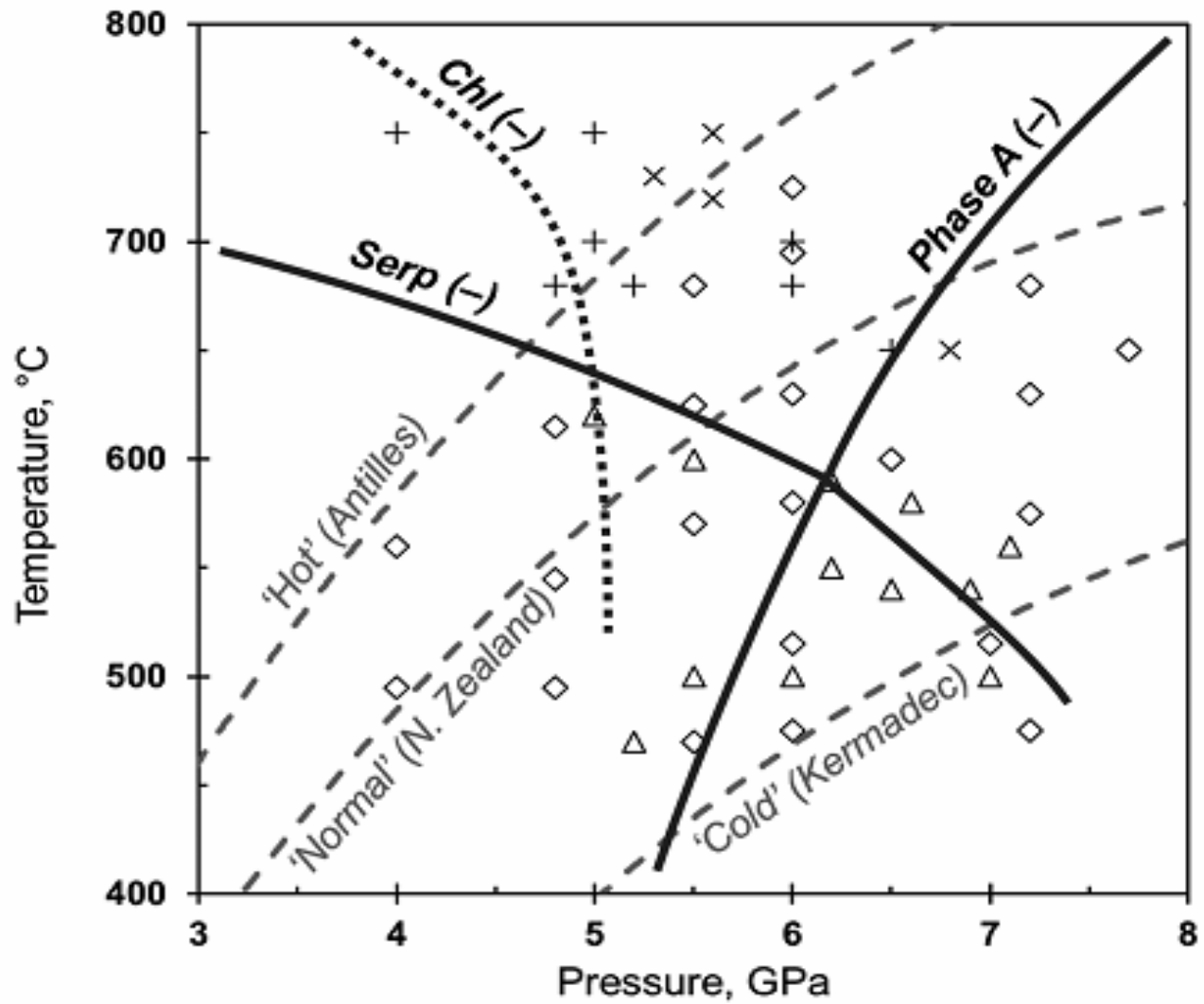


Fig. P-T phase diagram of serpentines at subduction conditions [9,24].

## Talc – TAP transformation at high P-T. Our data [24].

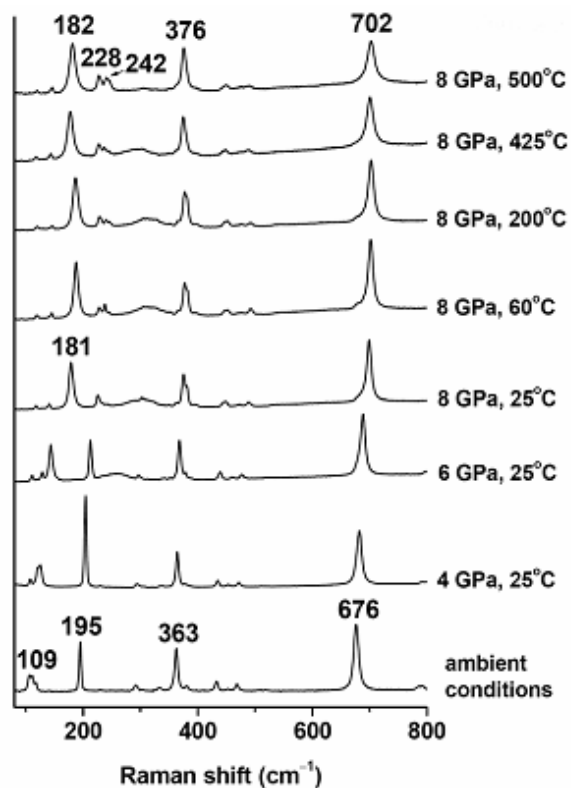


FIGURE 2. Raman spectra of *talc* +  $H_2O$  sample in the lattice-mode region collected during pressure and temperature increase from ambient conditions to 8 GPa/500 °C.

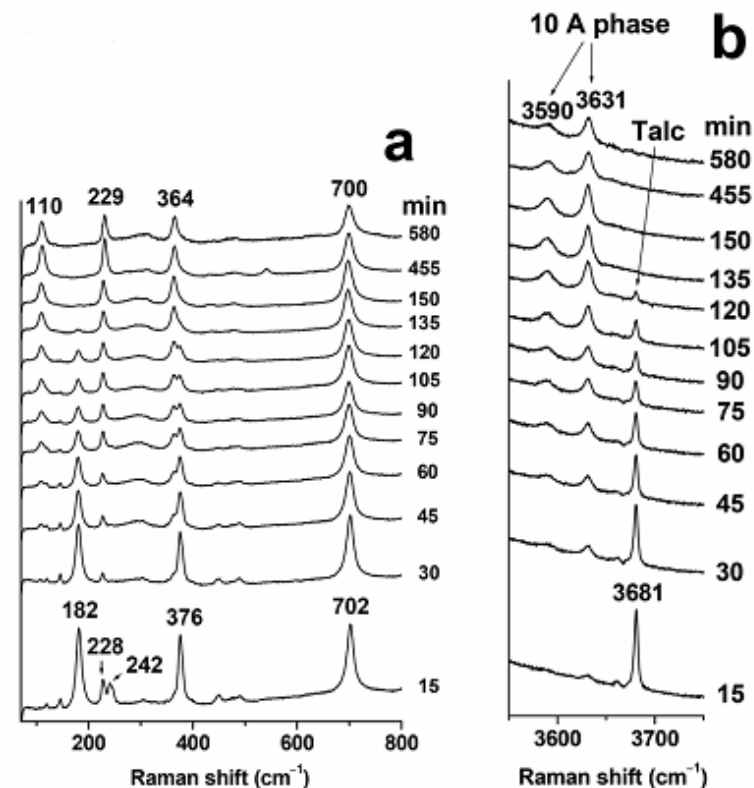
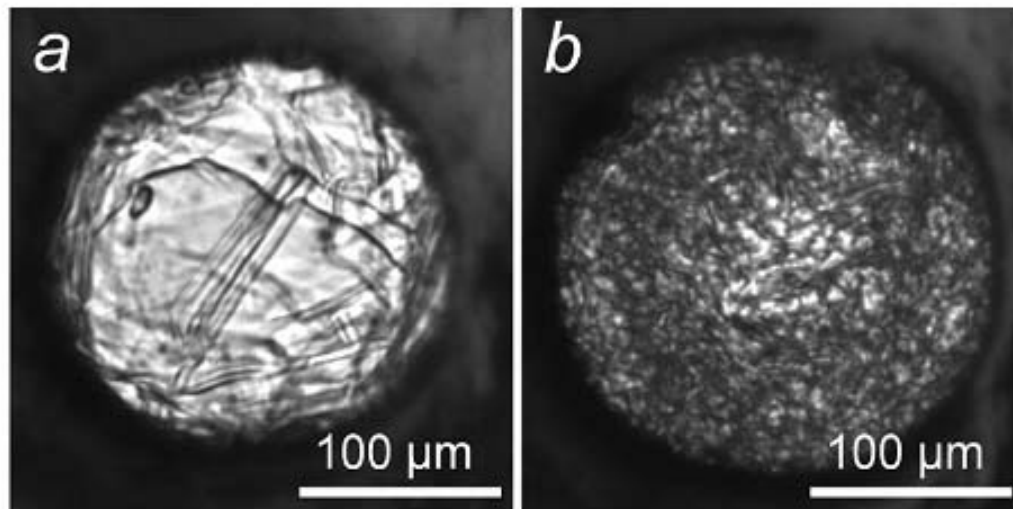


FIGURE 3. Raman spectra demonstrating *talc* +  $H_2O$   $\rightarrow$  10 Å phase reaction process in (a) lattice-mode region and (b) O-H stretching region. Timing start corresponds to the achievement of 8 GPa/500 °C conditions.



Talc – TAP  
transformation [24].

**FIGURE 4.** The sample at 8 GPa/500 °C before (a) and after (b) *talc* +  $H_2O \rightarrow 10 \text{ \AA}$  phase transformation.

### ABSTRACT

The synthesis of 10 Å phase via the reaction of talc plus water at 8 GPa and 500 °C was studied by in situ Raman spectroscopy using a diamond-anvil cell. The initial fast (2 h) incorporation of interlayer  $H_2O$  molecules into the talc structure is traced by gradual growth of new OH stretching bands at 3592 and 3621  $cm^{-1}$  and the shift of several framework bands. Further monitoring at HP-HT conditions over 7 h reveals gradual weakening of the 3592  $cm^{-1}$  band, which can probably be related to the onset of the formation of “long-run” 10 Å phase through the appearance of silanol groups following the model proposed by Pawley et al. (2010), influencing the interlayer hydrogen bonding.

Wairakite zeolite and OH-carbonate dawsonite at high P-T [26].

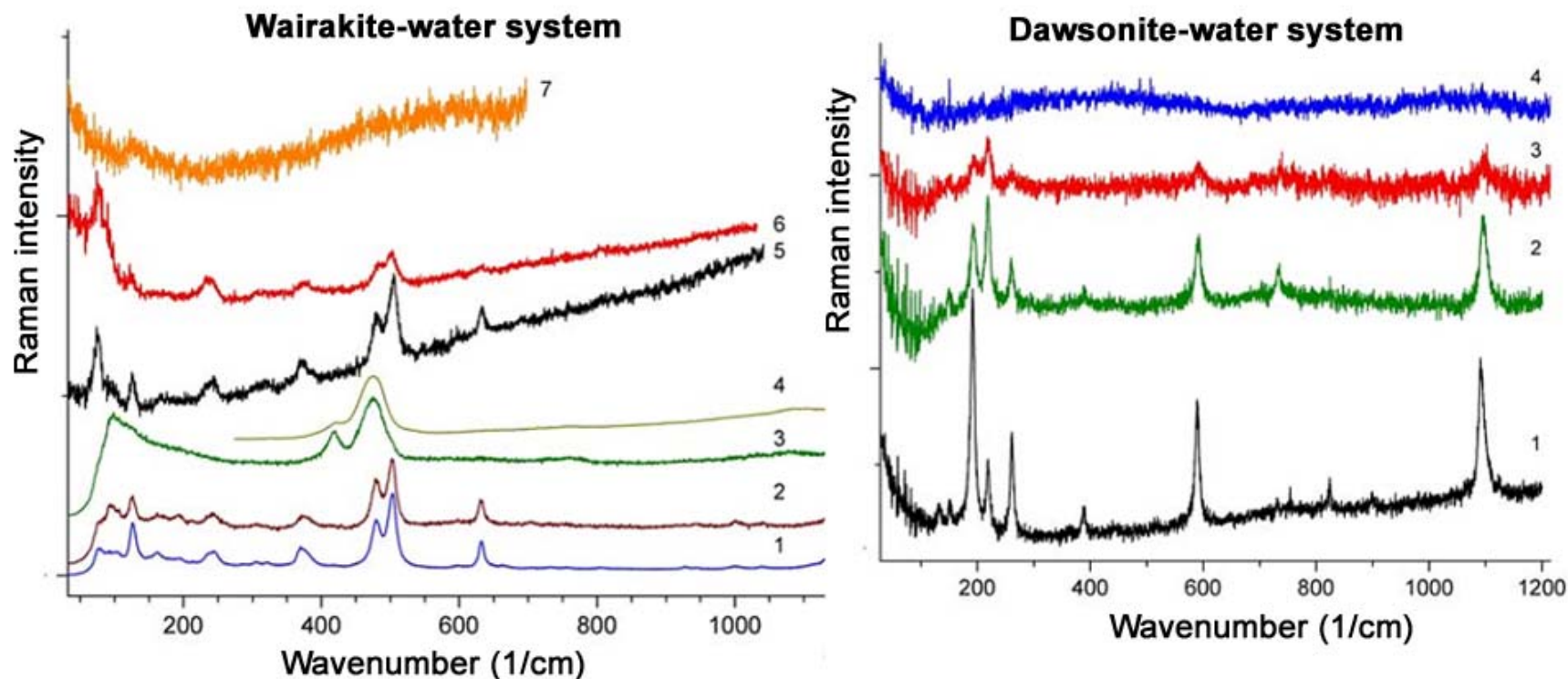


**Fig. (left).** Raman spectra obtained in the wairakite–water system at different P–T parameters: (1) 1 bar, 293 K as the initial temperature; (2) 1 bar, 293 K for wairakite after the experiment; (3) 1 bar, 293 K for phillipsite after the experiment in the wairakite–water system; (4) natural Ca–phillipsite; and wairakite compressed in a water medium in DAC at (5) 0.14 GPa, 293 K, (6) 0.37 GPa, 523 K and (7) 0.95 GPa, 673 K.

**Fig. (right).** Raman spectra of dawsonite compressed in a water medium at different P–T parameters: (1) 0.23 GPa, 295 K; (2) 0.47 GPa, 473 K; (3) 0.65 GPa, 573 K; and (4) 0.95 GPa, 723 K.



# Structure of thaumasite

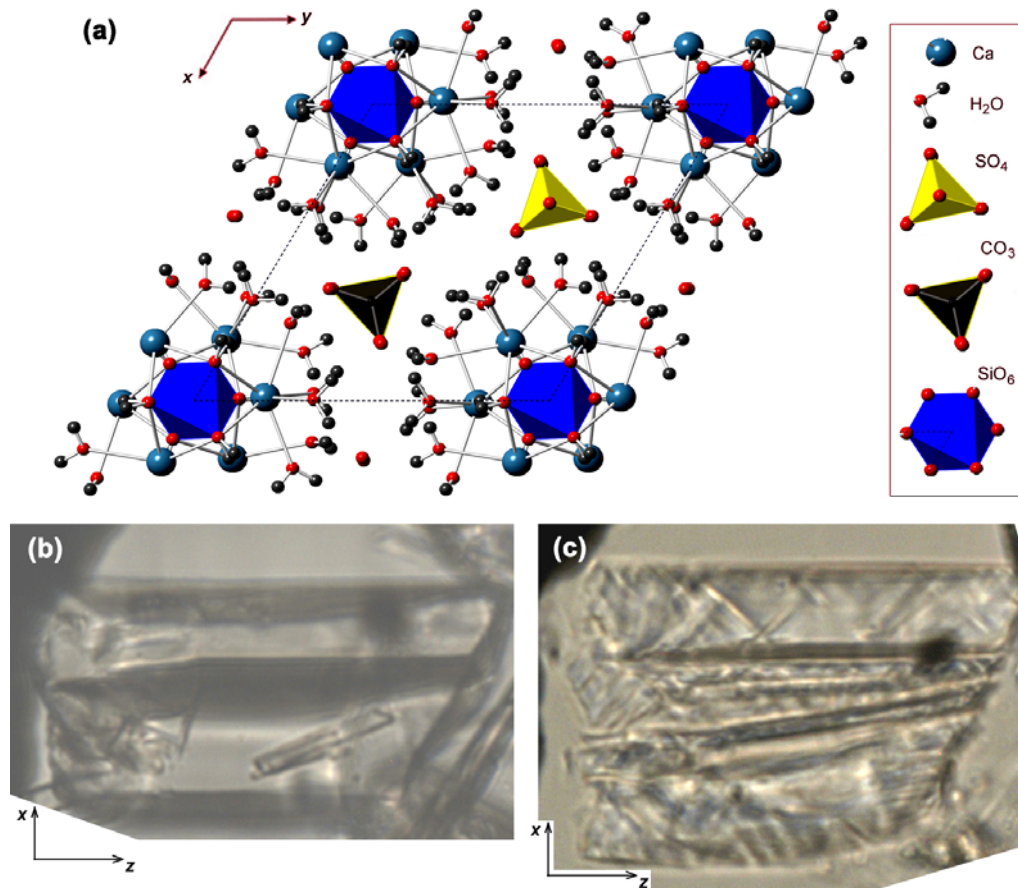


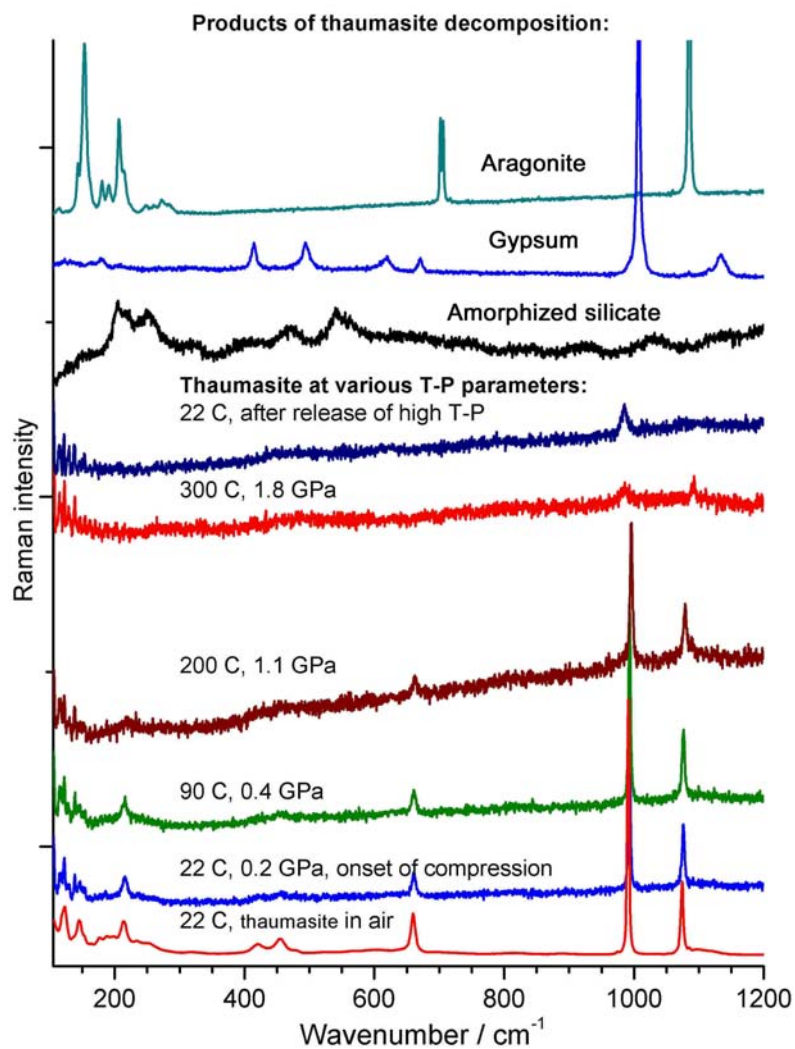
Figure 1. (a) The idealized crystal structure of thaumasite  $\text{Ca}_3\text{Si}(\text{OH})_6(\text{SO}_4)(\text{CO}_3) \cdot 12\text{H}_2\text{O}$  at room conditions. Groups of thaumasite Ca, SiO<sub>6</sub>, SO<sub>4</sub>, CO<sub>3</sub> and H<sub>2</sub>O, where SiO<sub>6</sub> polyhedron is a part of Si(OH)<sub>6</sub>, are plotted with CrystalMaker software.

(b) View of crystalline thaumasite I at water-alcohol pressure of 0.33 GPa (size of 94x170  $\mu\text{m}^2$  along  $xz$ ).

(c) View of the same crystalline phase-II thaumasite block at water-alcohol pressure of 4.6 GPa (Goryainov, J. Raman Spec. 2016) [28].

\* Previous data on thaumasite are available in ref. [1-6].

*Figure. In-situ and ex-situ Raman spectra of thaumasite compressed in water at high P-T*



## – Remarks on the P-T study of thaumasite

- In the present Raman study [28], thaumasite samples were compressed in distilled water, alcohol-water and KBr media at high pressures up to ~7 GPa: several phase transformations were identified. In samples compressed in alcohol-water, the wavenumbers of intense Raman bands of S-O and C-O symmetric stretching vibrations at 991 and 1074  $\text{cm}^{-1}$  proved to exhibit similar dependences on P: during first transition I→II at 4.4 GPa, the wavenumbers of both bands exhibited downward jump; at second transition II→III, which occurred at 4.9 GPa, each band split in doublet and, then at third transition III→IV at 5.4 GPa each doublet band transformed in singlet. In KBr medium, Raman bands of thaumasite showed similar (as at compression in alcohol-water) dependences on P.
- Transitions are assumed to be polymorphic: no noticeable overhydration in thaumasite compressed in water-alcohol occurred. In phase IV, gradual widening and weakening of each band were observed that is associated with amorphization.
- Considerable hysteresis was observed at thaumasite decompression. No overhydration of thaumasite was observed.
- Decomposition of thaumasite compressed in water is observed at 300 C, ~5 GPa. It transforms to aragonite + gypsum + (X-silicate) + fluid.
- After this HP-HT treatment, there is also remnant crystalline thaumasite having partially disordered structure.

- **CONCLUSION**

- **Method of in-situ Raman spectroscopy is effective tool to study the processes in minerals at high P:**
  - - **determination of the P-range of crystalline stability; polymorphic transitions;**
  - - **overhydration-hydration-dehydration at compression in water-containing medium;**
  - - **disordering and amorphization.**
- **Method at high P-T conditions:**
  - - **dissolution of the crystals;**
  - - **recrystallization of initial phase and growth of new crystalline phases;**
  - - **extraction of volatile components;**
  - - **large variety of other processes.**

## References

- [1] Ardit M., Cruciani G., Dondi M., Garbarino G.L., Nestola F. Phase transitions during compression of thaumasite,  $\text{Ca}_3\text{Si}(\text{OH})_6(\text{CO}_3)(\text{SO}_4)\cdot 12\text{H}_2\text{O}$ : A high-pressure synchrotron powder X-ray diffraction study // *Mineralogical Magazine*, October 2014. V. 78(5). P. 1193–1208.
- [2] Gatta, G.D., McIntyre, G.J., Swanson, J.G., Jacobsen, S.D. Minerals in cement chemistry: A single-crystal neutron diffraction and Raman spectroscopic study of thaumasite,  $\text{Ca}_3\text{Si}(\text{OH})_6(\text{CO}_3)(\text{SO}_4)\cdot 12\text{H}_2\text{O}$ . *American Mineralogist*, 2012, 97, 1060-1069.
- [3] Barnett, S. J.; C. D. Adam; A. R. W. Jackson. Solid solutions between ettringite,  $\text{Ca}_6\text{Al}_2(\text{SO}_4)_3(\text{OH})_{12}\cdot 26\text{H}_2\text{O}$ , and thaumasite,  $\text{Ca}_3\text{SiSO}_4\text{CO}_3(\text{OH})_6\cdot 12\text{H}_2\text{O}$ . *Journal of Materials Science*, 2000, 35 (16): 4109–4114.
- [4] Barnett, S. J.; D. E. Macphee; E. E. Lachowski; N. J. Crammond. XRD, EDX and IR analysis of solid solutions between thaumasite and ettringite. *Cement and Concrete Research.*, May 2002, 32 (5), 719-730.
- [5] Martucci, A. and Cruciani, G. In situ time resolved synchrotron powder diffraction study of thaumasite. *Physics and Chemistry of Minerals*, 2006, 33, 723-731.
- [6] V.A. Drebuschak, Yu.V. Seryotkin, S.N. Kokh, E.V. Sokol. Natural specimen of triple solid solution ettringite-thaumasite-chromate-ettringite. *J. Therm. Anal. Calorim.* 2013, 114, 777–783.
- [7] S.V. Goryainov, A.S. Krylov, Yu. Pan, I.A. Madyukov, M.B. Smirnov, A.N. Vtyurin. Raman investigation of hydrostatic and nonhydrostatic compressions of OH- and F-apophyllites up to 8 GPa. *Journal of Raman Spectroscopy*. 2012. V. 43. P. 439–447.
- [8] Goryainov S.V., Krylov A.S., Vtyurin A.N., Pan Y. Raman study of datolite  $\text{CaBSiO}_4(\text{OH})$  at simultaneously high pressure and high temperature // *J. Raman Spectrosc.* 2015, 46, 177–181.
- [9]. Schmidt M.W., Poli S. Generation of mobile components during subduction of oceanic crust. In: *Treatise on Geochemistry*. (Ed. R.L. Rudnick). Elsevier, 2003. V. 3. P. 567-591.
- [10]. Moroz N.K., Kholopov E.V., Belitsky I.A., Fursenko B.A. Pressure-enhanced molecular self-diffusion in microporous solids. *Microporous Mesoporous Mater.* 2001. V. 42. P. 113-119.
- [11] Lee Y., Vogt T., Hriljac J.A., Parise J.B., Hanson J.C., Kim S.J. Non-framework cation migration and irreversible pressure-induced hydration in a zeolite. *Nature*. 2002. V. 420. P. 485-489.
- [12] Seryotkin Y.V., Bakakin V.V., Fursenko B.A., Belitsky I.A., Joswig W., Radaelli P.G. Structural evolution of natrolite during over-hydration: a high-pressure neutron diffraction study. *Eur. J. Mineral.* 2005. V. 17. P. 305–313.
- [13] S.V. Goryainov, A.S. Krylov, A.Yu. Likhacheva, A.N. Vtyurin. Raman investigation of fibrous zeolites of natrolite group at high pressure of water medium.// *Bulletin of the Russian Academy of Sciences: Physics*. 2012. Vol. 76, N 7. P. 804-807.
- [14]. A.Yu. Likhacheva, S.V. Goryainov, A.S. Krylov, T.A. Bul'bak, P.S.R. Prasad. Raman spectroscopy of natural cordierite at high water pressure up to 5 GPa.// *Journal of Raman Spectroscopy*. 2012. V. 43. Iss. 4. P. 559–563.
- [15] Goryainov S.V., Secco R.A., Huang Y., Likhacheva A.Y. Pressure-induced ionic conductivity of overhydrated zeolite NaA at different water/zeolite ratios// *Microporous Mesoporous Mater.* 2013. V. 171. P. 125–130.
- [16] Lee Y., Hriljac J.A., Vogt T. Pressure-induced migration of zeolitic water in laumontite. *Phys.Chem.Min.* 2004. V.41, 421-428.

## References (continued)

- [17] S.V. Goryainov. A model of phase transitions in double-well Morse potential: Application to hydrogen bond.// *Physica B*. 2012. V. 407. P. 4233–4237.
- [18] Sherman W.F. Pressure-induced changes in mode Grüneisen parameters and general equations of state for solids // *Journal of Physics C: Solid State Physics*. 1982. V.15. P. 9-23; Sherman W.F. Vibrational spectroscopy under high pressures // *Bulletin de la Societe Chimique de France*. 1982. No. 9-10. P. I-347–I-369.
- [19] Likhacheva A.Yu., Goryainov S.V., Madyukov I. A., Manakov A.Yu., Ancharov A.I. Powder diffraction and Raman spectroscopic study of lawsonite at high water pressure.// *Bulletin of the Russian Academy of Sciences: Physics*, 2009, 73, № 8. P. 1143-1146.
- [20] Goryainov S.V., Krylov A.S., Vtyurin A.N. Behavior of natrolite zeolite and fluorapatite at high pressures in a water medium // *Bulletin of the Russian Academy of Sciences. Physics*. 2013, Vol. 77, No. 3, pp. 313–316.
- [21] Khoury H.N., Sokol E.V., Kokh S.N., Seryotkin Yu.V., Nigmatulina E.N., Goryainov S.V., Belogub E.V., Clark I.D. Tululite,  $\text{Ca}_{14}(\text{Fe}^{3+}, \text{Al})(\text{Al}, \text{Zn}, \text{Fe}^{3+}, \text{Si}, \text{P}, \text{Mn}, \text{Mg})_{15}\text{O}_{36}$ : a new Ca zincate-aluminate from combustion metamorphic marbles, central Jordan.// *Mineralogy and Petrology*. 2016. V. 110 (1). P. 125–140.
- [22] Khoury H.N., Sokol E.V., Kokh S.N., Seryotkin Yu.V., Kozmenko O.A., Goryainov S.V., Clark I.D. Intermediate members of the lime-monteponite solid solutions ( $\text{Ca}_{1-x}\text{Cd}_x\text{O}$ ,  $x = 0.36-0.55$ ): Discovery in natural occurrence.// *American Mineralogist*, 2016. V. 101. P. 132-147.
- [23] Sokol E.V., Kokh S.N., Khoury H.N., Seryotkin Yu.V., Goryainov S.V. Long-term immobilisation of  $\text{Cd}^{2+}$  at the Tulul Al Hammam natural analogue site, central Jordan.// *Applied Geochemistry*. 2016. V. 70. P. 43-60.
- [24] Rashchenko S.V., Likhacheva A.Yu., Goryainov S.V., Krylov A.S., Litasov K.D. In situ spectroscopic study of water intercalation into talc: New features of  $10 \text{ \AA}$  phase formation.// *American Mineralogist*, 2016. V. 101. P. 431–436.
- [25] Likhacheva A.Yu., Goryainov S.V., Seryotkin Yu.V., Litasov K.D., Momma K. Raman spectroscopy of chibaite, natural MTN silica clathrate, at high pressure up to 8 GPa. // *Microporous and Mesoporous Materials*. 2016. V. 224. P. 100-106.
- [26] S.V. Goryainov, A.S. Krylov, A.N. Vtyurin, A.Yu. Likhacheva, P.S.R. Prasad. In situ Raman study of wairakite and dawsonite interaction with water at high P–T parameters.// *Bulletin of the Russian Academy of Sciences. Physics*, 2016. V. 80, No. 5. P. 522–524.
- [27] Daniel, I., Fiquet, G., Gillet, P., Schmidt, M.W., Hanfland M., High-pressure behaviour of lawsonite: a phase transition at 8.6 GPa.// *Eur. J. Miner.*, 2000, 12, 721-733.
- [28] Goryainov S.V. Raman study of thaumasite  $\text{Ca}_3\text{Si}(\text{OH})_6(\text{SO}_4)(\text{CO}_3) \cdot 12\text{H}_2\text{O}$  at high pressure.// *Journal of Raman Spectroscopy*. 2016. V. 47. P. 984–992.
- [29] S.V. Goryainov, Y. Pan, M.B. Smirnov, W. Sun, J.-X. Mi. Raman investigation on the behavior of parasibirskite  $\text{CaHBO}_3$  at high pressure.// *Spectrochimica Acta Part A: Molecular and Biomolecular Spectroscopy*. 2017. V. 173. P. 46–52.

**Acknowledgements.** This work was supported by the Russian Science Foundation (Grant No. 15-17-30012).